

pubs.acs.org/est Article

Anthropogenic Forcing of the Baltic Sea Thallium Cycle

Chadlin M. Ostrander,* Yunchao Shu, Sune G. Nielsen, Olaf Dellwig, Jerzy Blusztajn, Heide N. Schulz-Vogt, Vera Hübner, and Colleen M. Hansel



Cite This: *Environ. Sci. Technol.* 2024, 58, 8510–8517



ACCESS I

Metrics & More

Article Recommendations

Supporting Information

ABSTRACT: Anthropogenic activities have fundamentally changed the chemistry of the Baltic Sea. According to results reported in this study, not even the thallium (TI) isotope cycle is immune to these activities. In the anoxic and sulfidic ("euxinic") East Gotland Basin today, TI and its two stable isotopes are cycled between waters and sediments as predicted based on studies of other redox-stratified basins (e.g., the Black Sea and Cariaco Trench). The Baltic seawater Tl isotope composition (ε^{205} Tl) is, however, higher than predicted based on the results of conservative mixing calculations. Data from a short sediment core from East Gotland Basin demonstrates that this high seawater ε^{205} Tl value originated sometime between about 1940 and 1947 CE, around the same time other prominent anthropogenic signatures begin to appear in the same core. This juxtaposition is unlikely to be coincidental and suggests that human activities in the surrounding area have altered the seawater Tl isotope mass-balance of the Baltic Sea.



KEYWORDS: thallium isotopes, Gotland Basin, euxinia

1. INTRODUCTION

The Baltic Sea is the largest anthropogenically induced hypoxic area on Earth. Hypoxic settings, also referred to as Dead Zones, are defined by bottom water dissolved oxygen (O₂) concentrations less than 2 mg L⁻¹, 1,2 The hydrography of the Baltic Sea makes it susceptible to hypoxia; North Atlantic seawater must pass two shallow sills before entering the semiisolated basin.^{3,4} Baltic seawater is brackish as a result, and has a near-permanent salt-gradient, or halocline, that prevents efficient mixing of surface and deep waters. Human activities have compounded these hydrographic effects since at least ~1950.5 Warming surface waters in the Baltic Sea negatively impact water column mixing and O2 solubility. And high nutrient loading drives eutrophication, in turn promoting large amounts of bottom water O2 consumption during microbial respiration. Deep basins are the locus of hypoxia in the central Baltic, most prominently those near the Islands of Bornholm, Fårö, and Gotland, as well as the Landsort Deep. Conditions are so reducing in some of these "deeps" that bottom waters are anoxic and rich in hydrogen sulfide (H2S), conditions referred to as "euxinic".8

Our focus in this investigation is the post-transition metal thallium (Tl). Thallium has a high toxicity: it is the most toxic metal for mammals, with an estimated minimal lethal dose for humans of 10 mg/kg. The bioavailability of Tl in nature therefore has important implications for human health. Some anthropogenic activities are strong point sources of Tl. An estimated ~2000 tons of Tl are released annually as atmospheric emissions during coal combustion, cement production, and pyrite roasting. 11,12 Due to its low melting

point, Tl is volatilized during these high-temperature processes and thereafter, upon cooling, condenses on the surface of ash particles. Ash produced during these anthropogenic processes can be highly enriched in Tl, by up to a factor of 10 compared to the raw materials. Thallium can accumulate to very high abundances in environments near anthropogenic point sources, greatly increasing the risk of Tl poisoning to neighboring communities.

We set out to better understand how Tl and its two stable isotopes, 203 Tl and 205 Tl, are today and were in the recent past cycled in the Baltic Sea. Thallium isotope ratio differences are reported in epsilon (ε) notation relative to the NIST–997 Tl standard as

$$\varepsilon^{205}\text{Tl} = (^{205/203}\text{Tl}_{\text{sample}} \div ^{205/203}\text{Tl}_{\text{NIST-997}} - 1)$$

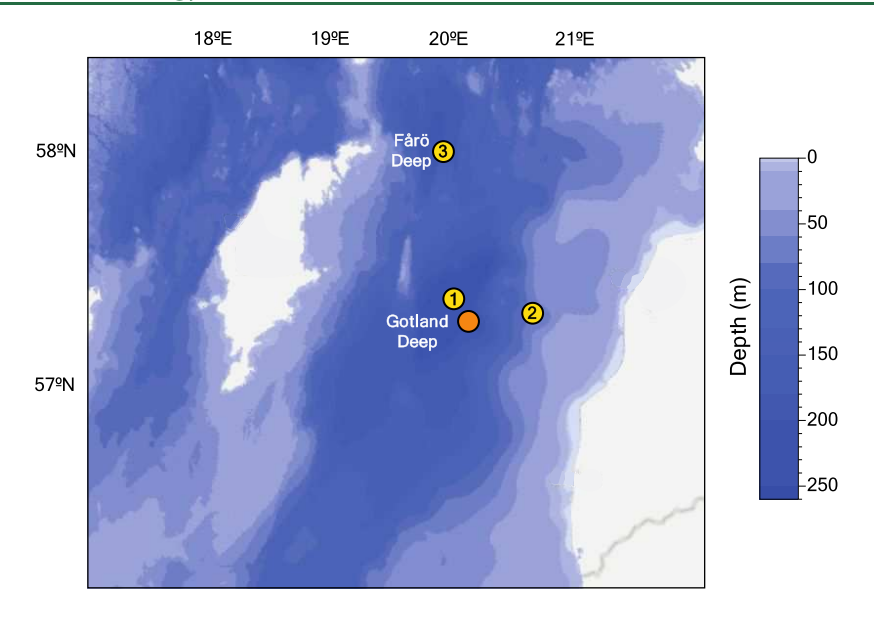
× 10, 000

Dissolved Tl abundances (Tl_{diss}) are very low in natural waters today, and especially low in anoxic waters where they average around 1 ng Tl L^{-1} . Accurate and precise Tl isotope ratio measurements require a few ng of Tl under typical analysis conditions, ¹⁸ which means that the collection of many liters of water is oftentimes required to generate

Received: February 8, 2024 Revised: April 17, 2024 Accepted: April 18, 2024 Published: May 2, 2024







Expedition	Station	Coordinates	Water depth (m)	Date (DDMMYYYY)
EMB201	7-4	57°16.980'N, 020°07.228'E	241	06122018
EMB276	1 TF271	57°11.520'N, 020°01.800'E	249	22092021
	② go24	57°16.000'N, 020°39.000'E	74	26092021
	3 go12	58°0.000'N, 019°54.000'E	203	23092021

Figure 1. Baltic Sea sampling locations and meta data.

reliable data. Because of these methodological challenges, very few studies to this point report dissolved Tl isotope ratio data for natural waters. $^{19-21}$ Especially few data exist for anoxic waters. 16,17

To help inform our understanding of modern Tl cycling, Tl concentration and isotope ratio data were generated for samples collected from the Baltic Sea during two expeditions aboard the research vessel Elisabeth Mann Borgese (Figure 1). According to these data, some of the same anthropogenic activities contributing to expanded Baltic Sea hypoxia play an important role in local Tl isotope mass-balance.

2. MATERIALS AND METHODS

Waters and sediments used for constraining the modern Tl cycle were collected at three stations during expedition EMB276 in September 2021. Sediments used for constraining the Tl cycle in the recent past were collected during expedition EMB201 in December 2018.

2.1. Sample Collection. High-volume water samples (\sim 10 L) were collected via free-flow water bottles (Hydro-Bios) at three stations in September 2021 during expedition EMB276: one station near the deepest point of the East Gotland Basin (TF271, 249 m water depth), one station on the eastern shelf of the East Gotland Basin (go24, 74 m water depth), and one station near the deepest point of the Fårö Deep (go12, 203 m water depth). Shortly after retrieval (no more than a few hours), each water sample was filtered using a precleaned sixposition Advantec PVC vacuum manifold equipped with 500 mL Nalgene funnels. Precleaned 0.22 μm pore size 47 mm poly(ether sulfone) (PES) membrane filters (Millipore) were used during filtering, and all water samples were acidified after filtering with twice-distilled trace metal free hydrochloric acid (HCl) to ~1 M HCl in preparation for ion exchange chromatography.

Sediments used to reconstruct modern Tl cycling were collected with a multicorer during expedition EMB276 at site TF271 in the East Gotland Basin. The short core from station TF271 was collected near the deepest point of the basin under euxinic conditions and is comprised of dark organic-rich sediments. This core was sampled at a three-centimeter resolution down to 17 cm sediment depth. All sediment samples collected during expedition EMB276 were frozen soon after collection and freeze-dried at Woods Hole Oceanographic Institution using a benchtop freeze-dryer with a polytetrafluoroethylene coated stainless steel collector (Labcono FreeZone). Once dry, each sample was ground to a fine powder using a FRITSCH Mini-Mill Pulverisette 23 with zirconium oxide bowl and grinding balls.

To reconstruct Tl cycling further back in time, the above-mentioned short core samples were supplemented with a longer sediment short core (45 cm sediment depth) collected near the deepest point of the East Gotland Basin in December 2018 during expedition EMB201 (core EMB201/7-4). Many complementary data are already published for this high-resolution core, including data that formulate a robust age model back to 1840 CE and data that track anthropogenic activities in the surrounding area of western Europe since this time. ²²

2.2. Water Column Redox Classification. Pump CTD profiles were taken and processed according to Schulz-Vogt et al. ²³ using electrochemical flow through sensors for oxygen and sulfide. The sensors were constructed at the Max Planck Institute for Marine Microbiology, Bremen (Microsensor group). Total sulfide was calculated using pH profiles detected with a flow through optode (Pyroscience GmbH, Aachen).

2.3. Metal Concentration Analyses. The contents of Al and Tl in the short core EMB201/7-4 were measured at IOW by inductively coupled plasma optical emission spectroscopy

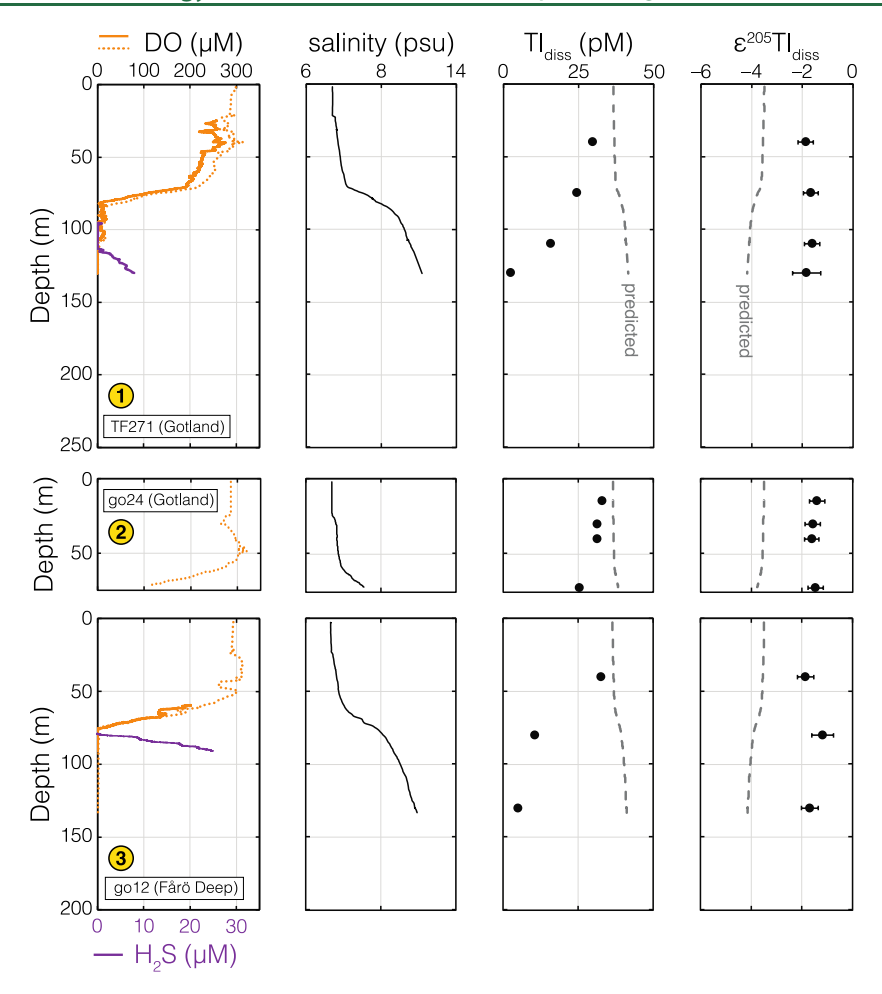


Figure 2. Water column data collected from three sampling stations during the EMB276 research cruise. Dashed dissolved oxygen (DO) profiles were collected via a SBE 911 plus CTD (Sea-Bird), while the solid DO and H_2S profiles were determined by microsensors attached to the pump CTD water flow. "Predicted" lines in the Tl data panels indicate the results of conservative salinity-based mixing calculations. Error bars associated with the Tl isotope ratio data indicate the 2SD sample reproducibility or the long-term standard reproducibility, whichever is greater.

(ICP-OES, iCAP 7400 Duo, Thermo Fisher Scientific) and inductively coupled plasma mass spectrometry (ICP-MS, iCAP Q, Thermo Fisher Scientific), respectively, after acid digestion of the freeze-dried and homogenized sediment material by a mixture of HNO₃–HF-HClO₄. Precision and trueness were checked by the international reference material TH-2 (NWRI) and were 3.4 and -2.0% for Al and 1.8 and 4.8% for Tl, respectively.

2.4. Thallium Isotope Analyses. Dried and finely powdered sediment samples were treated with dilute nitric acid (2 M HNO₃) on a hot plate overnight in perfluoroalkoxy alkane (PFA) vials (Savillex). This treatment is shown in previous work to effectively isolate authigenic (i.e., seawaterderived) Tl bound primarily to pyrite from Tl hosted in detrital minerals. After treatment, authigenic Tl was separated from detrital Tl by centrifugation and thereafter digested with a series of high-strength acid attacks (e.g., aqua regia, inverse aqua regia, concentrated HNO₃ + H_2O_2). To avoid the inadvertent inclusion of quantifiably important amounts of detrital-bound Tl, at no point was hydrofluoric acid (HF) used in the digestion process. Once completely digested, each sample was reconstituted in 1 M HCl in preparation for ion exchange chromatography.

All samples targeted for Tl isotope ratio analysis were purified following the typical two-step ion exchange chromatography protocol. 18,26 For the high-volume water column samples, this protocol was upscaled with larger capacity glassware custom manufactured for these sample types.

Thallium isotope ratio measurements were performed following procedures outlined in previous work using a Thermo Finnigan Neptune multicollector inductively coupled plasma mass spectrometer (MC-ICP-MS) located at the WHOI Plasma Mass Spectrometry Facility. A desolvating nebulizer system was used during sample introduction (Aridus II) and measurements were performed in low-resolution mode using sample-standard bracketing and external normalization to NIST SRM 981 Pb. NIST SRM 997 was used as the bracketing standard; all ε^{205} Tl data are calculated relative to this standard. Because each sample was doped with a known quantity of NIST SRM 981 Pb, authigenic Tl concentrations could be calculated during MC-ICP-MS analysis using measured 205Tl/208Pb ratios. All samples were analyzed in duplicate. The average and maximum 2 standard deviation (SD) reproducibility of these duplicate measurements was 0.2 and 0.8 ε units. One USGS shale SCo-1 standard was leached, purified, and analyzed with each sediment sample set to monitor accuracy. This standard yielded a $\varepsilon^{205} Tl_A$ value of -3.3 ± 0.6 ; 2SD (n = 4), which is indistinguishable from values reported in previous work ($\varepsilon^{205}\text{Tl}_A = -2.9 \pm 0.1$;

2SD²⁷). Reported errors are always in 2SD and either equal to the individual sample's reproducibility or the SCo-1 reproducibility, whichever is greater.

3. RESULTS AND DISCUSSION

Dissolved Tl profiles are nearly identical at all three stations: Tl_{diss} decrease with depth and dissolved isotope compositions ($\varepsilon^{205}Tl_{diss}$) are invariant (Figure 2). Dissolved Tl concentrations are as high as 33 pM in well-oxygenated surface waters and as low as 2 pM in sulfide-bearing waters below the oxycline. All $\varepsilon^{205}Tl_{diss}$ values are indistinguishable outside of error, averaging -1.6 ± 0.4 ; 2SD (n = 11).

In the core consisting of dark organic-rich sediment collected from the currently euxinic East Gotland Basin at Station TF271 (Figure 3), the concentration of authigenic Tl (Tl_A) leached from sedimentary sulfides averages 1.7 μ g/g \pm 1.3; 2SD (n = 6). Authigenic Tl isotope compositions (ε^{205} Tl_A) for the same samples average -1.3 ± 0.6 ; 2SD,

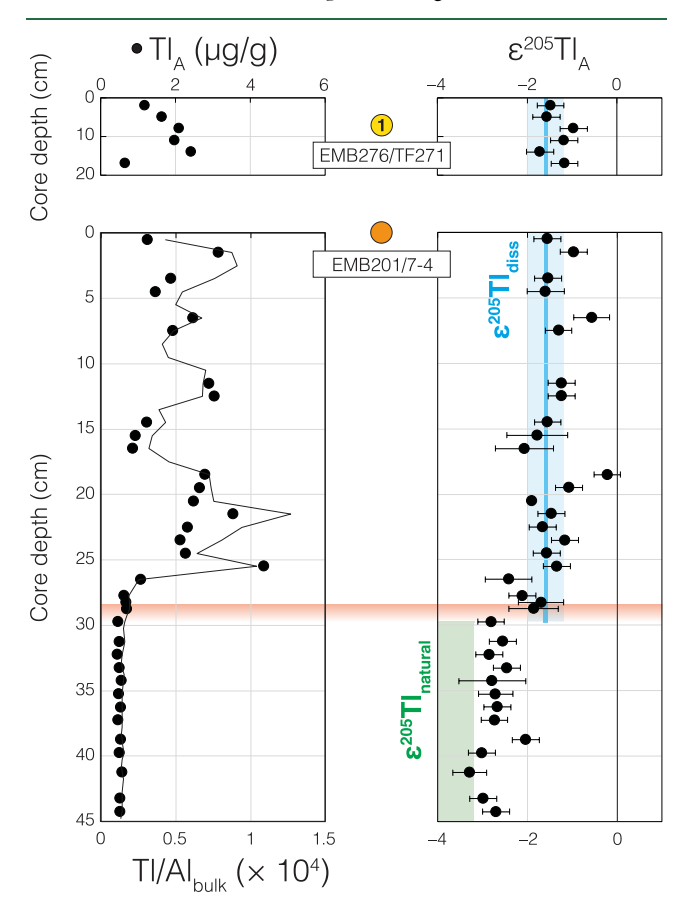


Figure 3. Sedimentary data tracking an abrupt change to the Baltic Sea Tl cycle since ~1940 CE. Data in the upper panels are from a short sediment core collected from the central Gotland basin during EMB276 (station TF271). Data in the lower panels are from a longer core collected nearby in the same basin during EMB201. Blue vertical shaded region signifies the average dissolved ε^{205} Tl value recovered from the water column in 2021. Green vertical shaded region signifies the calculated "natural" water column value assuming conservative mixing and a seawater salinity between 6 and 11 g kg $^{-1}$ (consistent with what is observed in East Gotland Basin; see Figure 2). Red gradient shaded region signifies the inferred transition period. Error bars associated with the Tl isotope ratio data indicate the 2SD sample reproducibility or the long-term standard reproducibility, whichever is greater.

within analytical uncertainty of the ε^{205} Tl_{diss} values measured in overlying waters (signified in blue in Figure 3).

In the EMB201/7-4 short sediment core above 29.75 cm depth, $\varepsilon^{205} Tl_A$ values are identical within error to those from sediments collected at site TF271 (Figure 3). At and below this depth, a striking and abrupt $\varepsilon^{205} Tl_A$ decrease is observed. The age of this transition is estimated as between ~1940 and ~1947 CE based on the respective inferred ages of the 29.75 cm depth horizon and the horizon sampled immediately above. An abrupt Tl_A change, mirrored in bulk sedimentary Tl/Al ratios (Tl/Al_{bulk}), is found at a slightly higher depth horizon of 26.5 cm with an estimated age of ~1956 CE. Authigenic $\varepsilon^{205}Tl$ average -1.5 ± 1.0 ; 2SD above 29.75 cm core depth, and -2.7 ± 0.6 ; 2SD at and below. Authigenic Tl concentrations average 2.2 $\mu g/g$ at and above 26.5 cm, and 0.5 $\mu g/g$ below.

3.1. Modern Baltic Sea Thallium Cycling. Today in the deeps of the East Gotland Basin, Tl and its two stable isotopes behave in a manner comparable to previously investigated euxinic basins. The rapid drawdown of Tl observed in the Baltic Sea water column in sulfidic waters below the oxycline is also observed under comparable conditions in the Black Sea, Cariaco Basin, and a small brackish pond on Cape Cod. As is the case in these other environments, interactions with sulfide minerals are most likely responsible for the rapid removal of Tl from the water column. Our study is the first to target multiple stations in a large anoxic basin, and our data resolution, while better than most previous investigations, is still low. Nonetheless, the homogeneous and conservative nature of our recovered ε^{205} Tl_{diss} values matches the behavior observed in the modern open ocean.

The behavior of Tl in recent sediments formed well below the oxycline in the central Gotland Basin is also comparable to what is observed in other euxinic settings. Namely, sulfide minerals that form in these sediments reliably capture the $arepsilon^{205}\mathrm{Tl}$ value of overlying waters. This is a finding replicated in all other anoxic basins studied to this point, ^{16,17,28,29} and even in productive upwelling zones where porewater O₂ penetration depths are shallow.²⁹ Seawater ε^{205} Tl capture in these locations implies some combination of near-quantitative Tl transfer to sediments 16 or partial transfer with no associated isotope fractionation. ¹⁷ Seawater ε^{205} Tl capture in EMB201/7-4 seems to have taken place even during short-lived Major Baltic Inflow events, or at least nearly so. Only a few minor sporadic shifts to higher $\varepsilon^{205} \text{Tl}_{\text{A}}$ values are found in the core, despite potential short-lived episodes of localized sedimentary Mn oxide burial during MBIs (perhaps up to +2 ε units in one sample aged to ~1978 CE).

Baltic seawater $\varepsilon^{205} Tl$ is, however, considerably higher than predicted based on conservative mixing (visible in Figure 2). Assuming binary mixing between open ocean seawater ($\varepsilon^{205} Tl = -6.0 \pm 0.3$; 2SD and $Tl_{\rm diss} = 65~{\rm pM}^{16}$) and natural freshwater sources ($\varepsilon^{205} Tl \approx -2.0$ and $Tl_{\rm diss} = 29~{\rm pM}^{20}$), the salinity of Baltic seawater dictates that it should have a $\varepsilon^{205} Tl$ value much closer to about $-3.6~\varepsilon$ units. The value we observe is about two ε units higher.

3.2. Baltic Sea Thallium Cycling in the Recent Past. Baltic seawater ε^{205} Tl has been higher than predicted since about 1940–1947 CE according to the EMB201/7-4 short sediment core (Figure 3). Seawater ε^{205} Tl capture seems likely throughout the core based on its high organic carbon contents, which requires persistent localized anoxia during sediment formation (TOC contents always exceed 3 wt $\%^{22}$). To iterate,

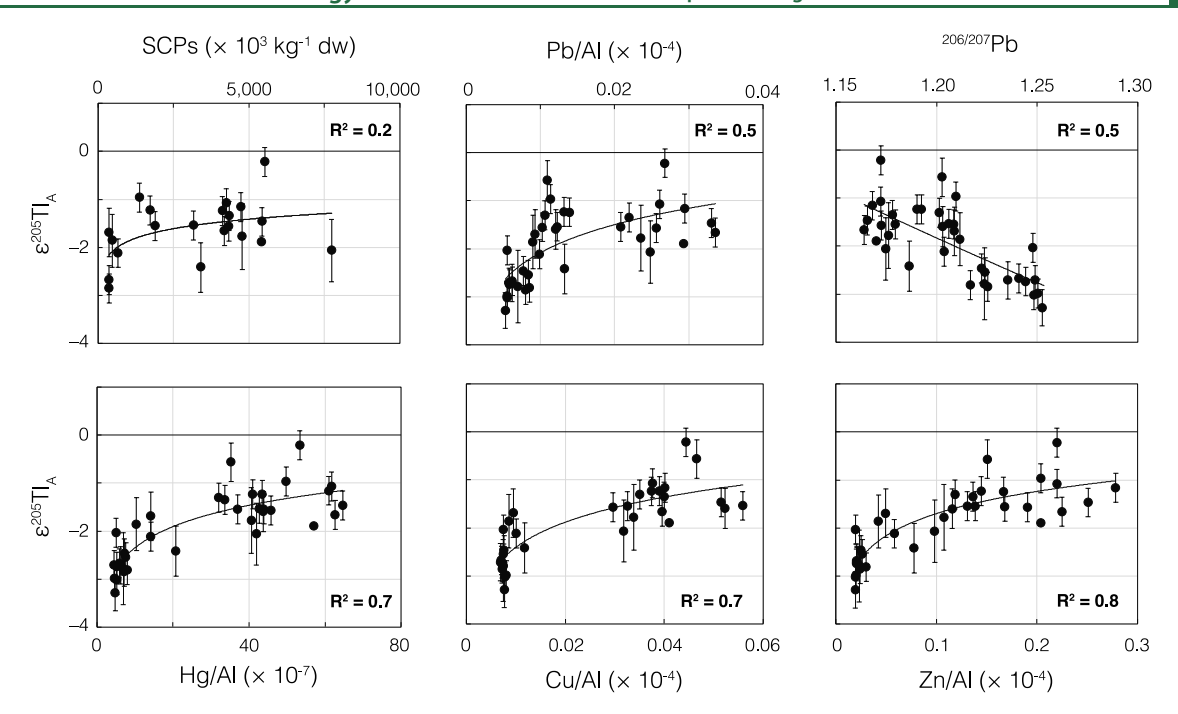


Figure 4. Correlations between Tl isotope ratios and anthropogenic geochemical markers from the EMB201/7-4 short sediment core. ²² All trendlines are logarithmic. Spheroidal carbonaceous fly ash particle (SCP) values of zero are omitted from the first panel. Error bars associated with the Tl isotope ratio data indicate the 2SD sample reproducibility or the long-term standard reproducibility, whichever is greater.

analogous sediments from the adjacent TF271 station forming under the same conditions capture the overlying seawater ε^{205} Tl value today, as do sediments forming under similar conditions in other locations worldwide. $^{16,1728-2930}$

To be sure, increased sedimentary Tl_A abundances above 26.5 cm core depth in the EMB201/7-4 short sediment core were supplemented by the development of strengthened euxinic conditions in the East Gotland Basin since the mid-1950s. Authigenic Tl concentrations increase by a factor of 4 in the EMB201/7-4 sediment core above this depth horizon, and this is despite a concurrent two factor increase in sedimentation rates. The net result of these changes is an 8-fold increase in sedimentary Tl accumulation rates in the central Gotland Basin. Sedimentary Tl accumulation is strongly linked to euxinia. Sedimentary Tl accumulation is strongly linked to euxinia. Accumulation contact that we rely instead on the slightly older ε^{205} Tl_A change as a more robust indicator of Baltic seawater Tl forcing.

The $\varepsilon^{205} Tl_A$ shift found in the EMB201/7-4 short sediment core is correlated with many other anthropogenic markers recovered from the same archive in previous work. The most direct evidence for increased anthropogenic inputs is a strongly elevated abundance of the coal combustion byproduct spheroidal carbonaceous fly ash particles (SCPs). These data are complemented by decreasing $^{206/207} Pb$ ratios and increasing Al-normalized ratios of Pb, Hg, Cu, and Zn (normalized to Al to minimize dilution effects caused by organic matter and high abundances of authigenic minerals), all of which can be attributed, at least in part, to anthropogenic activities in the area and worldwide strongly increasing in the 1950s.

It would be highly coincidental if the $\varepsilon^{205} Tl_A$ increase found in the EMB201/7-4 sediment core was not associated with the nearly contemporaneous trends linked to anthropogenic activities. The $\varepsilon^{205} Tl_A$ values are strongly correlated with these trends (Figure 4). The Baltic Sea Tl cycle changed in a measurable way starting around 1940–1947 CE. Barring

coincidence, the most parsimonious driver was anthropogenic pollution.

Alternative interpretations of the EMB201/7-4 data do exist, but none are more convincing. An influx of continental detritus with high $\varepsilon^{205} {\rm Tl}$ values could theoretically explain the observed isotopic shift. However, and paradoxically, higher ${\rm Tl/Al_{bulk}}$ ratios in this uppermost portion of the core would seem to indicate a smaller contribution from Al-rich detritus (Figure 3). Authigenic, seawater-derived Tl comprises the overwhelming fraction of Tl in these younger samples, especially after $\sim\!1956$ CE. In theory, Baltic seawater $\varepsilon^{205} {\rm Tl}$ could have increased because of the introduction of an output in the basin with a preference for the lighter-mass Tl isotope ($^{203} {\rm Tl}$). However, the long seawater residence time in the Baltic Sea of 26–29 years complicates this hypothesis. 32 The $\varepsilon^{205} {\rm Tl_A}$ increase found in the EMB201/7-4 core occurs over a much shorter time frame, perhaps as rapid as just a few years.

Release of isotopically heavy Tl from sediments during Mn oxide dissolution might also help explain the high Baltic seawater ε^{205} Tl values. In sediments formed beneath oxygenated bottom waters but with anoxic porewaters, Mn oxide minerals can form (and reform) near the sediment-water interface, but ultimately evade long-term burial because they are unstable under the reducing conditions deeper in the sediment pile.^{33–35} Thallium can be released back into the water column during this process, 36,37 and the expectation is that this Tl would be enriched in the heavier-mass isotope. 19 However, to explain the consistently high seawater ε^{205} Tl value since ~1940, Mn oxide dissolution (and thereby supply of Tl via this pathway) would have needed to occur at a quasiconstant rate for the last ~70 years. This scenario seems highly unlikely given the large disturbances to the Mn cycle observed in the Baltic Sea over the same time frame.^{4,31}

3.3. Quantifying and Identifying an Anthropogenic TI Source. What fraction of the Tl delivered to the Baltic Sea today and in the recent past comes from anthropogenic

pollutants? While a lack of data precludes precise quantification, there is reason to suspect that anthropogenic point sources have supplied a significant amount of Tl to the Baltic Sea since ~1940 CE — perhaps even the majority. The ε^{205} Tl value of the primary anthropogenic pollutant, if it were known, would allow for a more quantitative contribution estimate. Consider the following two-component mixing equation

$$\begin{split} \varepsilon^{205} & \text{Tl}_{\text{natural}}(f_{\text{natural}}) + \varepsilon^{205} & \text{Tl}_{\text{pollutant}}(f_{\text{pollutant}}) \\ &= \varepsilon^{205} & \text{Tl}_{\text{measured}} \end{split}$$

where $\varepsilon^{205} Tl_{natural}$ signifies the Tl isotope composition of natural Baltic seawater (estimated via salinity and assuming conservative mixing), $\varepsilon^{205} Tl_{pollutant}$ signifies the Tl isotope composition of the pollutant, $\varepsilon^{205} Tl_{measured}$ signifies the Tl isotope composition of Baltic seawater today, and f_X signify the fractions of natural and pollutant Tl in Baltic seawater. We perform the calculations using $\varepsilon^{205} Tl_{natural}$ values of -3.3 and -4.0, corresponding to a Baltic seawater salinity between about 6 and 11 g kg $^{-1}$ (consistent with what is observed in East Gotland Basin; Figure 2). Reassuringly, this range of $\varepsilon^{205} Tl_{natural}$ values is similar to what is found in the EMB201/7-4 core before \sim 1940, when anthropogenic Tl inputs were much less prominent (green shaded region in Figure 3). As summarized in Figure 5, the fraction of Tl in

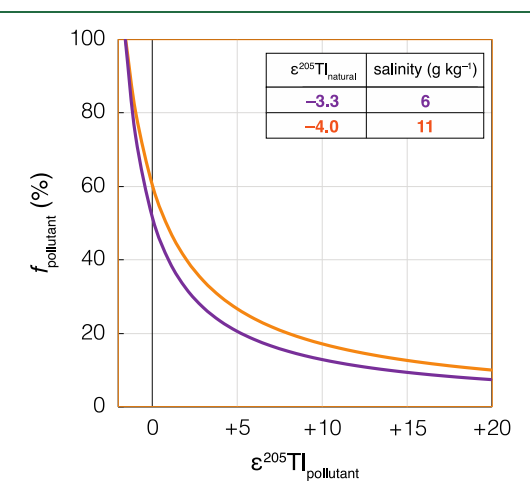


Figure 5. Percentage fraction of Baltic seawater Tl coming from anthropogenic pollutants for a given pollutant ε^{205} Tl value. Two calculations are performed, with only minor change in the results: one assuming a Baltic seawater salinity of 6 g kg⁻¹ (purple line) and another assuming a salinity of 11 g kg⁻¹ (orange line).

Baltic seawater from anthropogenic pollutants negatively correlates with the $\varepsilon^{205} Tl_{\rm pollutant}$ value; a lower $\varepsilon^{205} Tl_{\rm pollutant}$ value corresponds to a higher fraction of Tl from pollutants, and vice versa. A reasonable suspicion is that the $\varepsilon^{205} Tl_{\rm pollutant}$ value is, at most, only slightly positive; anthropogenically sourced Tl in materials analyzed to this point rarely exceed +5 ε units. 38 If this suspicion is correct, then more than $\sim\!20\%$ of the Tl delivered to the Baltic Sea comes from anthropogenic sources.

What is the identity of the primary anthropogenic pollutant? The answer to this question is complicated by unique Tl isotopic ratios for individual anthropogenic sources and phases. ^{39,40} Targeted work is ultimately required to test the various possibilities. However, there is reason to think that regional cement production may play an important role.

According to ice-core data from the French alps, together with past coal emission data and the results of atmospheric aerosol transport modeling, atmospheric Tl emissions from coal burning in the region were especially high between ~1920 and 1965. This time frame precedes the positive $\varepsilon^{205} Tl_A$ shift found in EMB201/7-4. Regional cement production, on the other hand, was enhanced considerably later, after the end of World War II and closer to the inferred age of the $\varepsilon^{205} Tl_A$ shift.41 Knowing the important role of cement production as an anthropogenic Tl source, 11,12 it is not unreasonable to assume that this process has introduced large amounts of Tl to the Baltic Sea. Cement kiln dust collected in the late 1970s from a cement plant near Lengerich, Germany has a $\varepsilon^{205} Tl$ value of -0.2 ± 0.4 . If anthropogenic Tl delivered to the Baltic Sea has a similar ε^{205} Tl value, then this would imply a substantial amount of Tl comes from this source, at least ~60%.

Despite seemingly large anthropogenic Tl inputs, the abundance of Tl in Baltic seawater today remains low and comparable to other natural bodies of water (a few to a few tens of pM⁴³). Sulfide accumulation plays a very important role in stunting Tl_{diss} accumulation, by efficiently stripping Tl from the water column below the oxycline. Notwithstanding, more Tl delivered to the Baltic Sea equates to a greater Tl toxicity risk. Bioaccumulation and biomagnification, for example, have the potential to concentrate Tl to more hazardous levels in fish at higher trophic levels, including those commonly consumed by humans (e.g., lake trout 44,45). If sulfidic conditions ever weaken in the Baltic Sea, for example because of more frequent inflow of oxygenated North Atlantic seawater,⁴ Tl would be less efficiently removed from the water column and also less likely to be retained in sediments. Both changes would lead to an increase in the size of the dissolved Baltic seawater Tl reservoir. An understanding of these dynamics will help improve predictive models of Tl cycling and availability in the face of continued climate change and anthropogenic forces.

ASSOCIATED CONTENT

Supporting Information

The Supporting Information is available free of charge at https://pubs.acs.org/doi/10.1021/acs.est.4c01487.

Dissolved thallium data collected during EMB276 Expedition (Table S1); sediment authigenic thallium data collected during EMB276 Expedition (Table S2); sediment data collected from the EMB201/7-4 short core (Table S3) (PDF)

AUTHOR INFORMATION

Corresponding Author

Chadlin M. Ostrander — Department of Marine Chemistry & Geochemistry, Woods Hole Oceanographic Institution, Woods Hole, Massachusetts 02543, United States; NIRVANA Laboratories, Woods Hole Oceanographic Institution, Woods Hole, Massachusetts 02543, United States; Present Address: Department of Geology & Geophysics, University of Utah, Salt Lake City, Utah 84112, United States; orcid.org/0000-0002-9119-5127; Email: chadlin.ostrander@utah.edu

Authors

Yunchao Shu — NIRVANA Laboratories and Department of Geology & Geophysics, Woods Hole Oceanographic

- Institution, Woods Hole, Massachusetts 02543, United States; Present Address: Department of Earth Sciences, University of Hong Kong, Pokfulam, Hong Kong 999077, China.
- Sune G. Nielsen NIRVANA Laboratories and Department of Geology & Geophysics, Woods Hole Oceanographic Institution, Woods Hole, Massachusetts 02543, United States; Present Address: CRPG, CNRS, Université de Lorraine, 54500 Nancy, France.
- Olaf Dellwig Department of Marine Geology, Leibniz Institute for Baltic Sea Research Warnemünde, IOW, 18119 Rostock, Germany
- Jerzy Blusztajn NIRVANA Laboratories and Department of Geology & Geophysics, Woods Hole Oceanographic Institution, Woods Hole, Massachusetts 02543, United States
- Heide N. Schulz-Vogt Department of Biological Oceanography, Leibniz Institute for Baltic Sea Research Warnemünde, IOW, 18119 Rostock, Germany
- Vera Hübner Microsensor Group, Max Planck Institute for Marine Microbiology, Bremen 28359, Germany
- Colleen M. Hansel Department of Marine Chemistry & Geochemistry, Woods Hole Oceanographic Institution, Woods Hole, Massachusetts 02543, United States; orcid.org/0000-0002-3506-7710

Complete contact information is available at: https://pubs.acs.org/10.1021/acs.est.4c01487

Author Contributions

C.M.O., S.G.N., O.D., and C.M.H. conceived the study. C.M.O. and C.M.H. collected samples during expedition EMB276. C.M.O., Y.S., O.D., H.N.S.-V., V.H., and J.B. performed geochemical analyses. C.M.O. wrote the paper, with input from S.G.N., O.D., J.B., H.N.S.-V., and C.M.H.

Notes

The authors declare no competing financial interest.

ACKNOWLEDGMENTS

We thank the crews and captains of RV Elisabeth Mann Borgese for their support during cruises EMB201 and EMB276. We thank Jérôme Kaiser and Maren Voss, the chief scientists of EMB201 and EMB276. Jérôme Kaiser is also thanked for providing sediment material from core EMB201/7-4. We thank Ann Dunlea for her assistance in solid sample preparation at Woods Hole Oceanographic Institution. We thank Maren Voss and Dirk de Beer for constructive comments on the original manuscript draft. C.M.O., S.G.N., and C.M.H. acknowledge support from National Science Foundation grant EAR-2129034. C.M.H. acknowledges support from National Science Foundation grant OCE-1924236. O.D. acknowledges funding by the Leibniz Association through grant SAW-2017-IOW-2649 (BaltRap).

REFERENCES

- (1) Gray, J. S.; Wu, R. S.; Or, Y. Y. Effects of hypoxia and organic enrichment on the coastal marine environment. *Mar. Ecol.: Prog. Ser.* **2002**, 238, 249–279.
- (2) Breitburg, D.; Levin, L. A.; Oschlies, A.; Grégoire, M.; Chavez, F. P.; Conley, D. J.; Garcon, V.; Gilbert, D.; Gutiérrez, D.; Isensee, K.; Jacinto, G. S.; Limburg, K. E.; Montes, I.; Naqvi, S. W. A.; Pitcher, G. C.; Rabalais, N. N.; Roman, M. R.; Rose, K. A.; Seibel, B. A.; Telszewski, M.; Yasuhara, M.; Zhang, J. Declining oxygen in the global ocean and coastal waters. *Science* **2018**, 359, No. eaam7240.

- (3) Fischer, H.; Matthäus, W. The importance of the Drogden Sill in the sound for major Baltic inflows. *J. Mar. Sci.* **1996**, *9*, 137–157.
- (4) Mohrholz, V. Major Baltic Inflow Statistics Revised. Front. Mar. Sci. 2018, 5, No. 384.
- (5) Carstensen, J.; Andersen, J. H.; Gustafsson, B. G.; Conley, D. J. Deoxygenation of the Baltic Sea during the last century. *Proc. Natl. Acad. Sci. U.S.A.* **2014**, *111*, 5628–5633.
- (6) Belkin, I. M. Rapid warming of large marine ecosystems. *Prog. Oceanogr.* **2009**, *81*, 207–213.
- (7) Conley, D. J.; Björck, S.; Bonsdorff, E.; Carstensen, J.; Destouni, G.; Gustafsson, B. G.; Hietanen, S.; Kortekaas, M.; Kuosa, H.; Meier, H. E. M.; Müller-Karulis, B.; Nordberg, K.; Norkko, A.; Nürnberg, G.; Pitkänen, H.; Rabalais, N. N.; Rosenberg, R.; Savchuk, O. P.; Slomp, C. P.; Voss, M.; Wulff, F.; Zillén, L. Hypoxia-related processes in the Baltic Sea. *Environ. Sci. Technol.* **2009**, *43*, 3412–3420.
- (8) Meyer, K. M.; Kump, L. R. Oceanic euxinia in Earth history: causes and consequences. *Annu. Rev. Earth Planet. Sci.* **2008**, *36*, 251–288.
- (9) Zitko, V. Toxicity and pollution potential of thallium. *Sci. Total Environ.* **1975**, *4*, 185–192.
- (10) Galván-Arzate, S.; Santamaría, A. Thallium toxicity. *Toxicol. Lett.* **1998**, 99, 1–13.
- (11) Pacyna, J. M.; Pacyna, E. G. An assessment of global and regional emissions of trace metals to the atmosphere from anthropogenic sources worldwide. *Environ. Rev.* **2001**, *9*, 269–298.
- (12) Antonia López Antón, M.; Spears, D. A.; Somoano, M. D.; Tarazona, M. R. M. Thallium in coal: Analysis and environmental implications. *Fuel* **2013**, *105*, 13–18.
- (13) Querol, X.; Fernández-Turiel, J.; López-Soler, A. Trace elements in coal and their behaviour during combustion in a large power station. *Fuel* **1995**, *74*, 331–343.
- (14) Karbowska, B. Presence of thallium in the environment: sources of contaminations, distribution and monitoring methods. *Environ. Monit. Assess.* **2016**, *188*, 640.
- (15) Peter, A. L. J.; Viraraghavan, T. Thallium: a review of public health and environmental concerns. *Environ. Int.* **2005**, *31*, 493–501.
- (16) Owens, J. D.; Nielsen, S. G.; Horner, T. J.; Ostrander, C. M.; Peterson, L. C. Thallium-isotopic compositions of euxinic sediments as a proxy for global manganese-oxide burial. *Geochim. Cosmochim. Acta* 2017, 213, 291–307.
- (17) Ostrander, C. M.; Nielsen, S. G.; Gadol, H. J.; Villarroel, L.; Wankel, S. D.; Horner, T. J.; Blusztajn, J.; Hansel, C. M. Thallium isotope cycling between waters, particles, and sediments across a redox gradient. *Geochim. Cosmochim. Acta* **2023**, 348, 397–409.
- (18) Nielsen, S. G.; Rehkämper, M.; Baker, J.; Halliday, A. N. The precise and accurate determination of thallium isotope compositions and concentrations for water samples by MC-ICPMS. *Chem. Geol.* **2004**, 204, 109–124.
- (19) Rehkämper, M.; Frank, M.; Hein, J. R.; Porcelli, D.; Halliday, A.; Ingri, J.; Liebetrau, V. Thallium isotope variations in seawater and hydrogenetic, diagenetic, and hydrothermal ferromanganese deposits. *Earth Planet. Sci. Lett.* **2002**, *197*, 65–81.
- (20) Nielsen, S. G.; Rehkämper, M.; Porcelli, D.; Andersson, P.; Halliday, A. N.; Swarzenski, P. W.; Latkoczy, C.; Günther, D. Thallium isotope composition of the upper continental crust and rivers an investigation of the continental sources of dissolved marine thallium. *Geochim. Cosmochim. Acta* **2005**, *69*, 2007—2019.
- (21) Nielsen, S. G.; Rehkämper, M.; Teagle, D. A. H.; Butterfield, D. A.; Alt, J. C.; Halliday, A. N. Hydrothermal fluid fluxes calculated from the isotopic mass balance of thallium in the ocean crust. *Earth Planet. Sci. Lett.* **2006**, *251*, 120–133.
- (22) Kaiser, J.; Abel, S.; Arz, H. W.; Cundy, A. B.; Dellwig, O.; Gaca, P.; Gerdts, G.; Hajdas, I.; Labrenz, M.; Milton, J. A.; Moros, M.; Primpke, S.; Roberts, S. L.; Rose, N. L.; Turner, S. D.; Voss, M.; do Sul, A. I. The East Gotland Basin (Baltic Sea) as a candidate Global Boundary Stratotype Section and Point for the Anthropocene series. *Anthropocene Rev.* **2023**, *10*, 25–48.
- (23) Schulz-Vogt, H. N.; Pollehne, F.; Jürgens, K.; Arz, H. W.; Beier, S.; Bahlo, R.; Dellwig, O.; Henkel, J. V.; Herlemann, D. P. R.; Krüger,

- S.; Leipe, T.; Schott, T. Effect of large magnetotactic bacteria with polyphosphate inclusions on the phosphate profile of the suboxic zone in the Black Sea. *ISME J.* **2019**, *13*, 1198–1208.
- (24) Dellwig, O.; Wegwerth, A.; Schnetger, B.; Schulz, H.; Arz, H. W. Dissimilar behaviors of the geochemical twins W and Mo in hypoxic-euxinic marine basins. *Earth-Sci. Rev.* **2019**, *193*, 1–23.
- (25) Nielsen, S. G.; Goff, M.; Hesselbo, S. P.; Jenkyns, H. C.; LaRowe, D. E.; Lee, C. A. Thallium isotopes in early diagenetic pyrite A paleoredox proxy? *Geochim. Cosmochim. Acta* **2011**, 75, 6690–6704.
- (26) Rehkämper, M.; Halliday, A. N. The precise measurement of Tl isotopic compositions by MC-ICPMS: application to the analysis of geological materials and meteorites. *Geochim. Cosmochim. Acta* **1999**, 63, 935–944.
- (27) Ostrander, C. M.; Owens, J. D.; Nielsen, S. G. Constraining the rate of oceanic deoxygenation leading up to a Cretaceous Oceanic Anoxic Event (OAE-2: ~ 94 Ma). *Sci. Adv.* **2017**, *3*, No. e1701020.
- (28) Fan, H.; Nielsen, S. G.; Owens, J. D.; Auro, M.; Shu, Y.; Hardisty, D. S.; Horner, T. J.; Bowman, C. N.; Young, S. A.; Wen, H. Constraining oceanic oxygenation during the Shuram excursion in South China using thallium isotopes. *Geobiology* **2020**, *18*, 348–365.
- (29) Chen, X.; Li, S.; Newby, S. M.; Lyons, T. W.; Wu, F.; Owens, J. D. Iron and manganese shuttle has no effect on sedimentary thallium and vanadium isotope signatures in Black Sea sediments. *Geochim. Cosmochim. Acta* 2022, 317, 218–233.
- (30) Wang, Y.; Lu, W.; Costa, K. M.; Nielsen, S. G. Beyond anoxia: exploring sedimentary thallium isotopes in paleo-redox reconstructions from a new core top collection. *Geochim. Cosmochim. Acta* **2022**, 333, 347–361.
- (31) Dellwig, O.; Wegwerth, A.; Arz, H. W. Anatomy of the Major Baltic Inflow in 2014: Impact of manganese and iron shuttling on phosphorus and trace metals in the Gotland Basin, Baltic Sea. *Cont. Shelf Res.* **2021**, 223, No. 104449.
- (32) Döös, K.; Meier, H. E. M.; Döscher, R. The Baltic haline conveyor belt or the overturning circulation and mixing in the Baltic. *Ambio: J. Hum., Environ.* **2004**, 33, 261–266.
- (33) Burdige, D. J. The biogeochemistry of manganese and iron reduction in marine sediments. *Earth-Sci. Rev.* **1993**, *35*, 249–284.
- (34) Calvert, S. E.; Pedersen, T. F. Sedimentary geochemistry of manganese: Implications for the environment of formation of manganiferous black shales. *Econ. Geol.* **1996**, *91*, 36–47.
- (35) Dellwig, O.; Schnetger, B.; Meyer, D.; Pollehne, F.; Häusler, K.; Arz, H. W. Impact of the Major Baltic Inflow in 2014 on Manganese Cycling in the Gotland Deep (Baltic Sea). *Front. Mar. Sci.* **2018**, *5*, No. 248.
- (36) Böning, P.; Schnetger, B.; Beck, M.; Brumsack, H. J. Thallium dynamics in the southern North Sea. *Geochim. Cosmochim. Acta* **2018**, 227, 143–155.
- (37) Ahrens, J.; Beck, M.; Böning, P.; Degenhardt, J.; Pahnke, K.; Schnetger, B.; Brumsack, H. Thallium cycling in pore waters of intertidal beach sediments. *Geochim. Cosmochim. Acta* **2021**, 306, 321–339.
- (38) Zhong, Q.; Qi, J.; Zi, J.; Liu, J.; Wang, J.; Lin, K.; Ouyang, Q.; Zhang, X.; Zhang, X.; Wei, X.; Wei, X.; Xiao, T.; Xiao, T.; El-Naggar, A.; El-Naggar, A.; Rinklebe, J. Thallium isotopic compositions as tracers in environmental studies: a review. *Environ. Int.* **2022**, *162*, No. 107148.
- (39) Vaněk, A.; Grösslova, Z.; Mihaljevič, M.; Trubač, J.; Ettler, V.; Teper, L.; Cabala, J.; Rohovec, J.; Zádorová, T.; Penížek, V.; Pavlu, L.; Holubík, O.; Nemeček, K.; Houška, J.; Drábek, O.; Ash, C. Isotopic tracing of thallium contamination in soils affected by emissions from coal-fired power plants. *Environ. Sci. Technol.* **2016**, *50*, 9864–9871.
- (40) Liu, J.; Yin, M.; Xiao, T.; Zhang, C.; Tsang, D. C. W.; Bao, Z.; Zhou, Y.; Chen, Y.; Luo, X.; Yuan, W.; Wang, J. Thallium isotopic fractionation in industrial process of pyrite smelting and environmental implications. *J. Hazard. Mater.* **2020**, 384, No. 121378.
- (41) Legrand, M.; McConnell, J. R.; Preunkert, S.; Bergametti, G.; Chellman, N. J.; Desboeufs, K.; Plach, A.; Stohl, A.; Eckhardt, S. Thallium pollution in Europe over the twentieth century recorded in

- Alpine ice: Contributions from coal burning and cement production. *Geophys. Res. Lett.* **2022**, 49, No. e2022GL098688.
- (42) Kersten, M.; Xiao, T.; Kreissig, K.; Brett, A.; Coles, B. J.; Rehkämper, M. Tracing anthropogenic thallium in soil using stable isotope compositions. *Environ. Sci. Technol.* **2014**, *48*, 9030–9036.
- (43) Belzile, N.; Chen, Y.-W. Thallium in the environment: a critical review focused on natural waters, soils, sediments and airborne particles. *Appl. Geochem.* **2017**, *84*, 218–243.
- (44) Lin, T.-S.; Nriagu, J.; Wang, X.-Q. Thallium concentration in Lake Trout from Lake Michigan. *Bull. Environ. Contam. Toxicol.* **2001**, 67, 921–925.
- (45) Nagel, A.; Cuss, C. W.; Goss, G. G.; Shotyk, W.; Glover, C. N. Accumulation of thallium in rainbow trout (*Oncorhynchus mykiss*) following acute and sub-chronic waterborne exposure. *Environ. Toxicol. Chem.* **2023**, 42, 1553–1563.